



# Effect of stigmasterol-based mesogen and phytosphingosine on the Langmuir monolayer of DPPC

S. Mahesha<sup>1</sup>, Gayathri Madhavankutty<sup>1</sup>, M. Neelanjana<sup>1</sup>, S. Vanishree Bhat<sup>2</sup>, Sandeep Kumar<sup>3</sup>, and Bharat Kumar<sup>1,a</sup> 

<sup>1</sup> Department of Physics, Central University of Karnataka, Kadaganchi, Kalaburagi, Karnataka 585367, India

<sup>2</sup> Soft Condensed Matter Group, Raman Research Institute, C. V. Raman Avenue, Bengaluru, Karnataka 560080, India

<sup>3</sup> Department of Chemistry, NITTE Meenakshi Institute of Technology (NMIT), Yelahanka, P. B. No. 6429, Bengaluru, Karnataka 560064, India

Received 13 December 2023 / Accepted 25 March 2024

© The Author(s), under exclusive licence to EDP Sciences, Springer-Verlag GmbH Germany, part of Springer Nature 2024

**Abstract** We have studied the effect of a novel stigmasterol-based mesogen (4-mercaptoalkyl benzoate of stigmasterol or 4MBS) and phytosphingosine (PHS molecules) on the Langmuir monolayer of 1, 2 dipalmitoyl-sn-glycero-3-phosphocholine (DPPC) using the surface manometry technique. The mixed monolayers of 4MBS/DPPC and PHS/DPPC in different compositions are investigated using surface manometry. The surface pressure–area per molecule isotherms were analysed to determine the mechanical and thermodynamical aspects like phase transitions and stability of the mixed Langmuir monolayer. The Brewster angle microscope (BAM) was used for visualising the monolayer morphology. Our studies show that PHS and 4MBS molecules stabilise the liquid expanded (LE)–liquid condensed (LC) phase coexistence region of the DPPC monolayer.

## 1 Introduction

The lipid bilayer membrane enclosing the biological cell and organelles plays a vital role in many physiological processes like signal transduction and cross-membrane transport [1]. The biological cell membrane comprises several components like phospholipids, sphingolipids, sterols, sugar and proteins. The relative composition of these components decides the properties of the cell membrane. Due to the complexity in terms of variety of components and their relative composition, it is challenging to study the role of each component towards the properties of cell membrane. Hence, the model membranes are preferred over cell membranes for controlled study [2].

Langmuir monolayer is a model system which mimics one of the two leaflets of a bilayer cell membrane. Langmuir monolayer can be described as a monomolecular thick film of amphiphilic molecules spontaneously formed at the air–water interface. Several studies have been carried out to understand the Langmuir monolayers of biological lipids [3–5]. Phospholipid molecules, considered to be the building blocks of a cell membrane, can form a stable monolayer [6]. 1, 2-dipalmitoyl-sn-glycero-3-phosphocholine (DPPC) is one of such molecules and an important component of the cell membrane [7, 8]. It is an important constituent of the lung surfactants that plays a vital role in avoiding the alveolar collapse [9, 10]. The characteristic feature of the DPPC Langmuir monolayer is the presence of coexistence region of the liquid expanded (LE) and liquid condensed (LC) phases [11, 12]. In this coexistence region, the ordered LC domain is dispersed in a disordered LE phase. The LE–LC coexistence region in the monolayer of DPPC has attracted many studies and the effect of other lipid molecules on the coexistence region of DPPC monolayer is of interest. The structure and the stability of coexistence of the ordered and disordered phases in a cell membrane depend on the membrane lipid composition. Studies have been carried out to understand the order–disorder phases and their stability using phosphatidylcholine lipids like DPPC [13].

The LE–LC transition is expected to be a first-order phase transition, where the  $\pi - A_m$  isotherm shows a plateau region with a zero slope in the coexistence region. In the DPPC monolayer, interestingly, the LE–LC

<sup>a</sup> e-mail: [bharat@cuk.ac.in](mailto:bharat@cuk.ac.in) (corresponding author)

coexistence regions have a non-zero slope in the  $\pi - A_m$  isotherm. Several studies were conducted to explain the nature and the genesis of the non-horizontal curve with a non-zero slope. Mohwald [6] et al. claimed the LE-to-LC transition to be a second order or “diffuse first order” phase transition and the transition region is characterised by a long-range orientational and short-range positional order of the molecules. Pallas et al. [14] and Hifeda et al. [15] attributed the non-horizontal slope to the presence of surface active impurities. Other studies attribute the non-horizontal coexistence curve to the consequence of formation of molecular aggregates like surface micelles [16, 17]. Arriga et al. [18] explained the observed mechanical properties of the monolayer by considering the energetics of phase transition and the mechanical properties of the coexisting phases. Eiji Hatta et al. [13] attributed the non-horizontal curve between LE and LC phases in the the  $\pi - A_m$  isotherm to the coupling between the lateral molecular density ( $\rho$ )-2D strain ( $\epsilon_s$ ) and to the collective chain tilt ( $\theta$ ). Raghavendra et al. [19] have studied the role of this coupling in the mixed monolayer of  $\gamma$ -Oryzanol and DPPC. The thermodynamic analysis would help in understanding the factors affecting the stability of the coexistence of order-disorder phases of multi-component monolayers. The effect of other lipids on the LE-LC coexistence region in the Langmuir monolayer of DPPC is not well understood and requires further investigations. Such studies may help in understanding the formation of ordered domains from the disordered region and the stability of their coexistence at higher composition of sterols [3, 20, 21].

In this article, the effects of a 4-mercaptododecyl benzoate of stigmaterol (4MBS) and the effect of sphingolipid phytosphingosine (PSP) on the DPPC monolayer and its LE-LC coexistence region in  $\pi - A_m$  isotherm are studied using the surface manometry technique. The stigmaterols are plant sterols [22], well known for their anti-carcinogenic properties [23]. These molecules have a hydrophobic rigid core compared to DPPC [24]. Phytosphingosine is known for preventing moisture loss and protecting the skin from environmental damage and also for anti-inflammatory and anti-microbial activities [25–28]. In order to understand the effect of stigmaterol derivative and sphingolipid on coexistence of the order and disordered phases in thin films containing phosphatidylcholine (PC) lipids, we have carried out experiments on mixed monolayers of DPPC-4MBS and DPPC-PHS using surface manometry technique. Our studies help in understanding the role of coupling between the lateral molecular density ( $\rho$ )-2D strain ( $\epsilon_s$ ) and to collective tilt ( $\theta$ ) on the stable coexistence of disordered LE-ordered LC phase in the Langmuir monolayer. Such studies may also help in understanding the properties of vesicle membranes formed by these mixtures.

## 2 Experimental details

### 2.1 Materials

DPPC was purchased from Avanti polar lipids and used without any further processing. The 4MBS was synthesised and characterised as described elsewhere [29, 30]. PHS was purchased from the Tokyo chemical industry (TCI). The stock solution of DPPC (1 mg/ml) and 4MBS (0.5 mg/ml) was prepared in HPLC-grade chloroform. The stock solution of PHS (0.9 mg/ml) was prepared in HPLC grade chloroform/methanol (9:1) methanol. The stock solutions of DPPC/4MBS and DPPC/PHS were prepared to get different mole fractions of 4MBS and PHS in DPPC, respectively, for further studies.

### 2.2 Methods

The surface manometry technique is employed for studying the  $\pi - A_m$  isotherms obtained using the KSV Nima trough (Fig. 1). Langmuir monolayers were formed by spreading the stock solutions using Hamilton micro-syringe on the subphase of ultra-pure deionised water (Evaqua; model: W3T324496). The isotherms were recorded at a temperature of  $24.0 \pm 0.5$  °C. All the experiments were carried out for atleast three times to check the reproducibility of the isotherms. The sensitivity of the tensiometer was  $0.01 \text{ mNm}^{-1}$  and the accuracy in area per molecule calculation was  $0.5 \text{ \AA}^2$ . The Brewster angle microscopy (BAM) images having a resolution of  $12 \mu\text{m}$ , are taken using the KSV Nima (Model: MicroBAM), equipped with a 50 mW laser source emitting a p-polarized light beam of wavelength 659 nm. The BAM images for surface pressure ( $\pi$ ) values taken at an interval of every  $0.5 \text{ mNm}^{-1}$  are analysed along with the  $\pi - A_m$  isotherms.

## 3 Results and discussion

The 4MBS/DPPC and PHS/DPPC mixtures do not form a stable monolayer at composition greater than 0.3 mole fraction of 4MBS and PHS in DPPC. For relative mole fractions of 0.1, 0.2 and 0.3, the mixed monolayer exhibits reproducible isotherms and BAM images. Figure 2 shows  $\pi - A_m$  isotherms of the mixed Langmuir monolayers of

**Fig. 1** Schematic representation of surface manometry technique

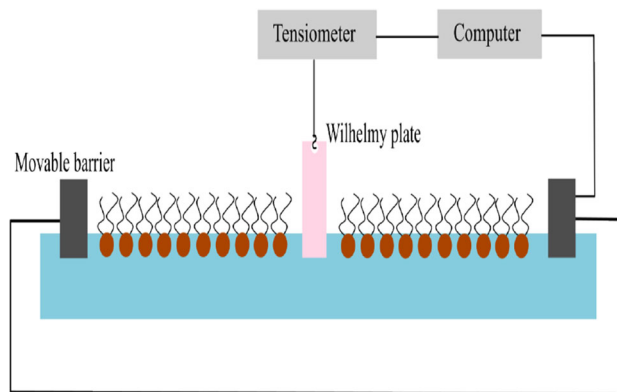
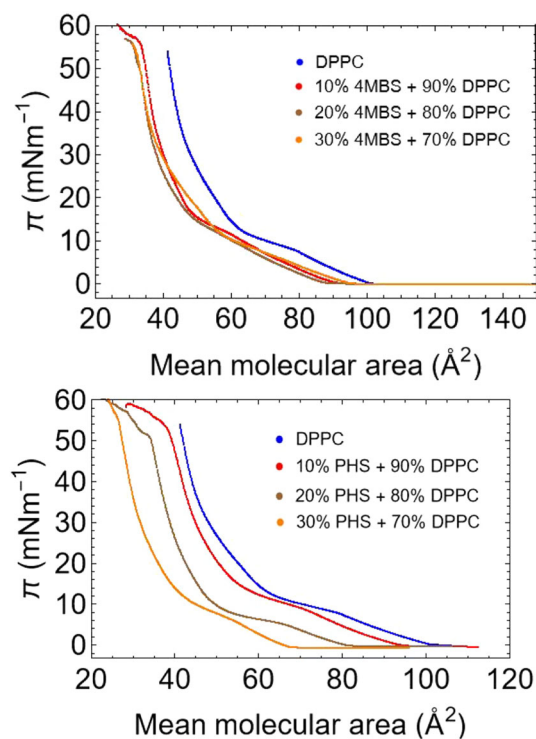


**Fig. 2**  $\pi - A_m$  isotherms of mixed monolayers of 4MBS/DPPC and PHS/DPPC for different mole fractions of 4MBS and PHS, respectively



DPPC/4MBS and DPPC/PHS systems. The mixed monolayers of 4MBS/DPPC have  $\pi - A_m$  isotherms shifted towards the lower  $A_m$  as compared to pure DPPC monolayer, irrespective of the relative composition. In the case of PHS/DPPC mixed monolayer (Fig. 2), the isotherms shift towards lower area per molecule and the extent of shift increases with the increasing PHS mole fraction.

The compression modulus of the monolayer can be obtained from the  $\pi - A_m$  isotherms using the equation [31]

$$|E| = A_m \frac{d\pi}{dA_m} \tag{1}$$

Smaller values of compression modulus correspond to the higher compressibility of the monolayer, indicating a less rigid phase. Similarly, the value of the modulus is higher for the condensed state of the monolayer and will have lower compressibility [32]. Figure 3 shows the variation of compression modulus as a function of area per molecule for different mole fraction of 4MBS and PHS in DPPC. The maximum of compression modulus ( $|E|_{Max}$ ) which corresponds to uniform LC phase shifts towards the lower  $A_m$  value as composition of 4MBS or PHS increases. It can be noted that the  $|E|_{Max}$  values decrease with the increasing 4MBS or PHS relative composition in the DPPC monolayer (Fig. 4). The variation of the collapse pressure  $\pi_c$  (the maximum surface pressure up to which the monolayer remains stable [33]) for different relative composition of 4MBS or PHS in the monolayer is shown in Fig. 4. The decrease in  $\pi_c$  with the increase in 4MBS composition up to 0.2 mole fraction indicates the decrease

**Fig. 3** Variation of compression moduli as a function of mean molecular area for different mole fraction of 4MBS and PHS in DPPC monolayer

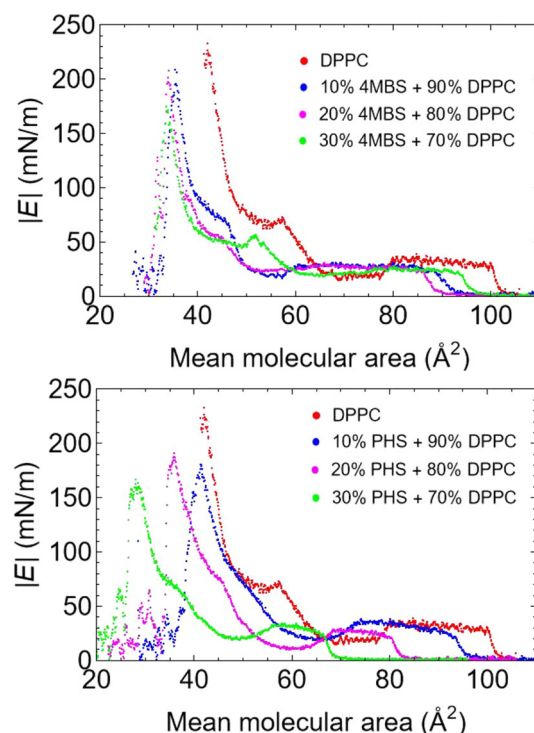
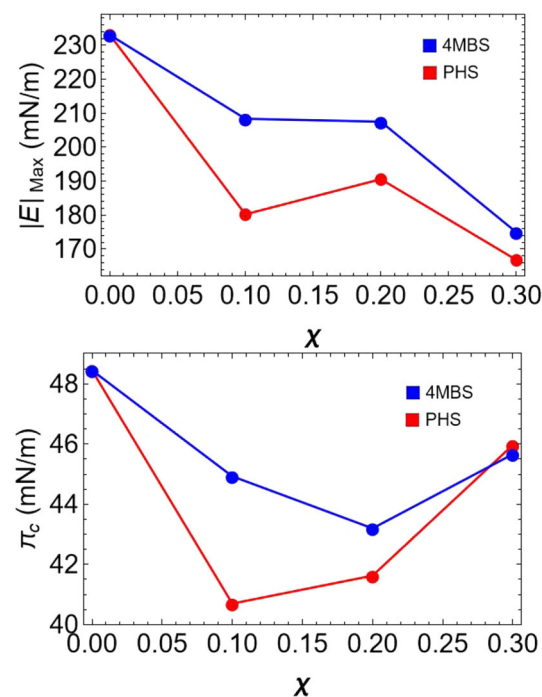


**Fig. 4** Plot of (a) maximum of compression moduli  $|E|_{Max}$  and (b) collapse pressure for different mole fractions of 4MBS and PHS in DPPC monolayer. Solid line is a cue to eye



in monolayer stability against the collapse state [34]. For PHS/DPPC mixture, the collapse pressure  $\pi_c$  decreases with increase in the PHS composition for 0.1 PHS mole fraction and it increases for  $\chi_{PHS}=0.2$  and  $\chi_{PHS}=0.3$ .

In the case of 4MBS/DPPC monolayer with  $\chi_{4MBS}=0.1$ , the range of LE-LC phase coexistence region decreases with respect to that of the pure DPPC monolayer. The liquid expanded phase is a low density phase where the average area per molecule is larger than the size of the hydrophilic head group [35]. On compressing the monolayer transforms to a more ordered liquid condensed (LC) phase and the liquid expanded to liquid condensed phase is characterised by a coexistence region. It is also observed that for higher compositions of 4MBS, the range of coexistence region increases with the increase in the 4MBS relative composition. This indicates that adding



4MBS stabilises the LE–LC coexistence region of DPPC monolayer. Addition of sterols like cholesterol to the phospholipid monolayer causes the reduction of LE–LC coexistence region [3, 36]. This difference can be due to the steric hindrance caused by the additional double bond in the hydrophobic side chain and the aromatic hydrophobic core in the sterol moiety [36, 37]. In the case of PHS/DPPC monolayer, the range of LE–LC phase coexistence is found to be decreasing as the mole fraction of PHS ( $\chi_{PHS}$ ) increases, showing a major difference of the effect of 4MBS from that of stigmasterol on DPPC monolayer. Our analysis shows that the isotherms are less reproducible for 4MBS or PHS mole fractions of more than 0.3 in the DPPC monolayer.

The visualisation of the phase transitions in the mixed monolayers is carried out using Brewster angle microscopy (BAM). The BAM images were recorded for every  $0.5 \text{ mNm}^{-1}$  interval of the surface pressure along with the isotherms. The reflectivity of a monolayer is a function of refractive index and is hence affected by the molecular packing and orientation of the molecules on the subphase. This change in reflectivity produces contrast in the images recorded. The BAM images of pure DPPC show a low reflecting homogeneous region corresponding to low surface density phases like gaseous (G) and LE phase [12]. On compression, bright multilobed LC domains of DPPC appear in the low reflecting LE phase when the monolayer starts transition from the low density LE phase to the high density LC phase. The appearance of curls in the same direction in the multilobed domains is attributed to the chirality of DPPC molecules [5, 38]. For higher surface pressures, the size of the multilobed LC domains increases on compression and at collapse the homogeneous condensed phase transforms to small 3D crystalline structures [39].

Different phases exhibited by the mixed monolayers of 4MBS/DPPC and PHS/DPPC can be characterised from BAM images (Fig. 5) and  $|E|$ – $A_m$  isotherms (Fig. 3). For mixed monolayer with 4MBS mole fraction of  $\chi_{4MBS} = 0.1$  in DPPC, the monolayer exhibited gaseous phase for area per molecule greater than  $91 \text{ \AA}^2$  and LE phase from  $91 \text{ \AA}^2$  to  $61 \text{ \AA}^2$ . The coexistence of LE–LC phases was between  $61 \text{ \AA}^2$  and  $50.5 \text{ \AA}^2$ . In this region BAM shows the existence of bright irregular LC domain in the dark LE region (Fig. 5a). On further compression the homogeneous bright LC region is observed from  $50.5 \text{ \AA}^2$  to  $36 \text{ \AA}^2$ . The monolayer collapsed at  $36 \text{ \AA}^2$  with collapse pressure of  $48 \text{ mNm}^{-1}$ . For the mixed monolayer of DPPC with PHS mole fraction of  $\chi_{PHS} = 0.1$  in DPPC (Fig. 2), the gaseous phase was observed for the area per molecule greater than  $94 \text{ \AA}^2$  and the LE phase from  $94 \text{ \AA}^2$  to  $71.5 \text{ \AA}^2$ . The LE–LC coexistence region was found to be between  $A_m$  of  $71.5 \text{ \AA}^2$  and  $58 \text{ \AA}^2$  (Fig. 5d). Further compression showed the uniform LC phase till  $38 \text{ \AA}^2$ . The monolayer collapsed at  $38 \text{ \AA}^2$  with a collapse pressure of  $\pi = 57.5 \text{ mNm}^{-1}$ . The BAM images of the pure DPPC monolayer show the growth of bean shaped LC domains to *S* –shaped, multi-lobed structures and finally circles [40].

For mixed monolayer having  $\chi_{4MBS} = 0.2$  (Fig. 2), the homogeneous gaseous phase is found above the mean molecular area  $88 \text{ \AA}^2$  and G - LE coexistence is observed from  $88 \text{ \AA}^2$  to  $85.5 \text{ \AA}^2$ . The monolayer was in the homogeneous LE phase from  $85.5 \text{ \AA}^2$  to  $62.5 \text{ \AA}^2$ . From  $62.5 \text{ \AA}^2$  to  $50 \text{ \AA}^2$ , the monolayer is found to be in the

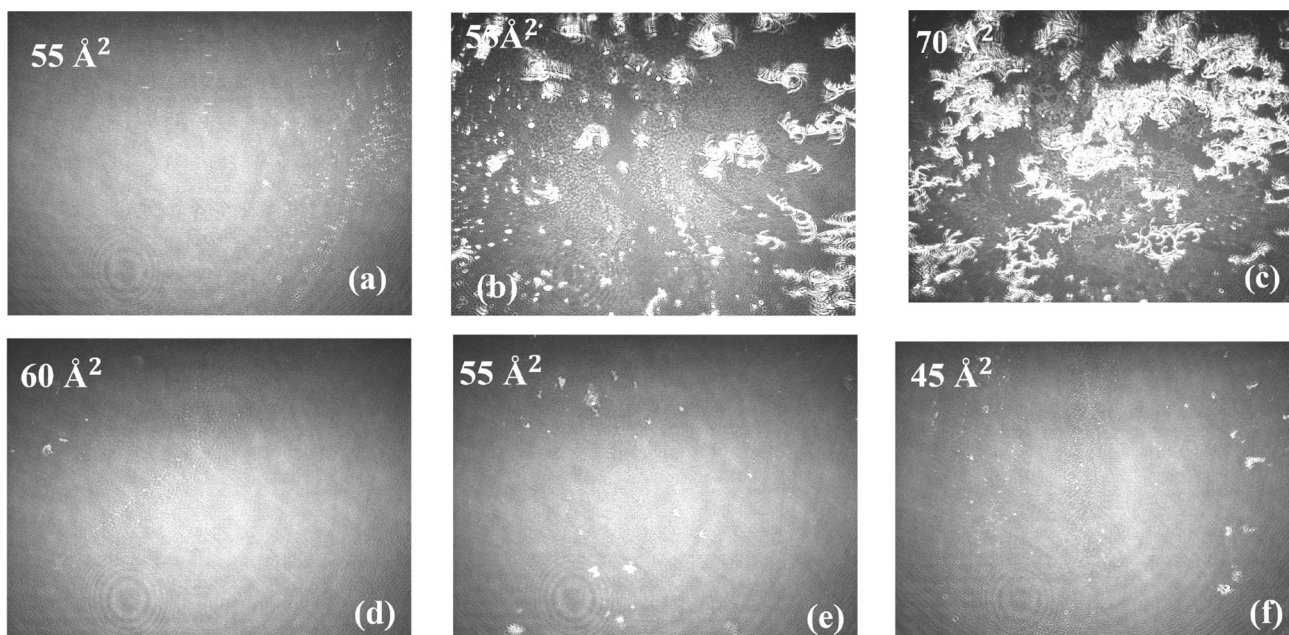


**Fig. 5** a, b and c show the BAM images for 4MBS/DPPC mixed monolayers in LE - LC coexistence region for  $\chi_{4MBS} = 0.1$ , 0.2 and 0.3, respectively. d, e and f show the BAM images for PHS/DPPC mixed monolayers in LE–LC coexistence region for  $\chi_{PHS} = 0.1$ , 0.2 and 0.3, respectively. The size of the images is  $3.6 \text{ mm} \times 4 \text{ mm}$

LE–LC coexistence phase with the increased number of multilobed LC domains (Fig. 5b). The multilobed domain are found to be persistent even in the uniform LC phase at  $50 \text{ \AA}^2$  to  $34 \text{ \AA}^2$ . The appearance of bright 3D crystallites signifies the collapse of the monolayer at  $34 \text{ \AA}^2$ . For mixed monolayer having  $\chi_{PHS} = 0.2$  (Fig. 2), the homogeneous gaseous phase is found above  $80 \text{ \AA}^2$  and LE phase is found from  $80 \text{ \AA}^2$  to  $66.5 \text{ \AA}^2$ . The LE–LC coexistence region (Fig. 5e) was observed from  $66.5 \text{ \AA}^2$  to  $52 \text{ \AA}^2$ . The uniform LC phase was exhibited from  $52 \text{ \AA}^2$  to  $32 \text{ \AA}^2$  and the monolayer finally collapsed at  $34 \text{ \AA}^2$  with a collapse pressure of  $50 \text{ mNm}^{-1}$ .

Similarly, for  $\chi_{4MBS} = 0.3$  (Fig. 2), the homogeneous gaseous phase was observed above  $93 \text{ \AA}^2$  and G - LE coexistence phase from  $93 \text{ \AA}^2$  to  $91 \text{ \AA}^2$ . The boundaries of the LE phase in the G–LE coexistence region were found to be more sharper than that in the G–LE coexistence phase of  $\chi_{4MBS} = 0.2$  mixed monolayer. This suggests that the 4MBS molecules in the mixed monolayer increases the density of the condensed phase. The monolayer was in the LE phase from  $91 \text{ \AA}^2$  to  $78 \text{ \AA}^2$  and from  $78 \text{ \AA}^2$  to  $60 \text{ \AA}^2$  the monolayer exhibited LE–LC coexistence region. BAM images of the coexistence region show the increased number of multilobed domains (Fig. 5c). The monolayer was in the LC phase from  $60 \text{ \AA}^2$  to  $33.5 \text{ \AA}^2$  before collapsing with the collapse pressure of  $47 \text{ mNm}^{-1}$ . For  $\chi_{PHS} = 0.3$  (Fig. 2), the homogeneous gaseous phase is observed above the mean molecular area of  $66 \text{ \AA}^2$  and LE phase from  $66 \text{ \AA}^2$  to  $54.5 \text{ \AA}^2$ . Further compression leads to LE–LC coexistence region from  $54.5 \text{ \AA}^2$  to  $40 \text{ \AA}^2$  (Fig. 5f). The monolayer exhibits LC phase from  $40 \text{ \AA}^2$  to  $26.1 \text{ \AA}^2$ . The monolayer collapsed at  $26 \text{ \AA}^2$  with a collapse pressure of  $\pi \approx 55 \text{ mNm}^{-1}$ .

In earlier studies, the bean shaped structures or bilobed structures in the BAM images are ascribed to more stable domain shape for DPPC molecules[41, 42]. The rise of multilobed structure is explained by considering the line tension and repulsive interactions between the DPPC molecules[43]. Monte Carlo simulation studies attributed these metastable multilobed structures to the thermal fluctuations in the system[44]. Analysing the BAM images of all the mixed monolayers (Fig. 5), it is found that the addition of 4MBS enhances the formation of multilobed DPPC domains while that of PHS inhibits its formation, indicating that both the molecules are present in the monolayer.

The width of the LE–LC coexistence region increases with the increase in the stigmasterol derivative 4MBS and sphingolipid PHS in the DPPC monolayer. On the other hand for 4MBS/DPPC monolayer, the range of  $A_m$  for LC phase increases and for LE phases decreases with increase in  $\chi_{4MBS}$ . In the case of PHS/DPPC mixed monolayers, the range of  $A_m$  for the coexistence region marginally increases with the increase in  $\chi_{PHS}$ . The range of mean molecular area corresponding to LE phase decreases with the increase in  $\chi_{PHS}$ , however, in contrast to the 4MBS/DPPC monolayer, the LC phase decreases. PHS molecules with strong polar head group are expected to be located with its head group in subphase. The presence of PHS molecules results in repulsive interactions between head groups and may result in increased  $A_m$  range for gas phase and reduced  $A_m$  range for LE phase.

To further understand the behaviour of the mixed monolayers, we have studied the miscibility and stability of the monolayer from the excess area ( $A_{ex}$ ) and excess Gibbs free energy ( $\Delta G_{ex}$ ) calculations. An ideal mixed monolayer or a monolayer having completely immiscible components follows the additivity rule described by the equation [45],

$$A_{ideal} = \chi_{DPPC} A_{DPPC} + \chi_x A_x \quad (2)$$

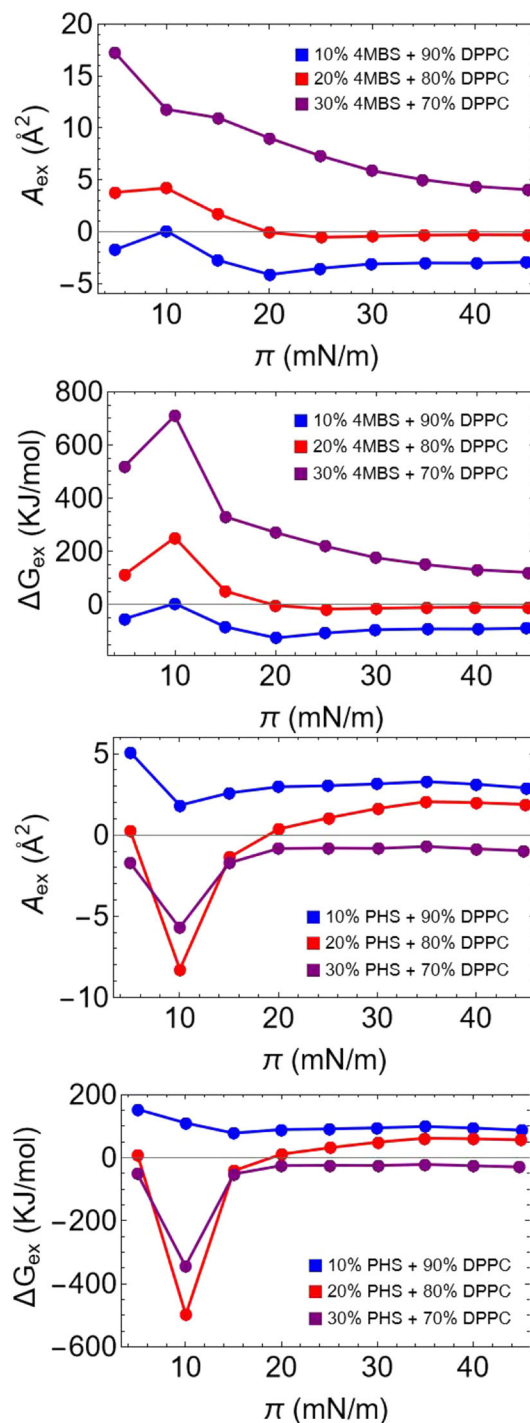
where,  $A_{ideal}$  is the area per molecule of the mixed monolayer at the given surface pressure,  $\pi^i$ ,  $\chi_{DPPC}$  and  $\chi_x$  are the mole fractions of the components DPPC and  $x$  respectively, and  $A_{DPPC}$  and  $A_x$  are the area per molecule of the DPPC and  $x$  at the surface pressure  $\pi^i$  respectively. The deviation of mean molecular area from the  $A_{ideal}$  is known as the excess area  $A_{ex}$  of the mixed monolayer is given by the equation [37, 45],

$$A_{ex} = A_{12} - A_{ideal} \quad (3)$$

Here,  $A_{12}$  is the mean molecular area of the mixed monolayer at the surface pressure  $\pi^i$ . For an ideal mixed monolayer, the  $A_{ex}$  will be zero. The inter-molecular interactions in any mixed monolayer are determined by the chemical structure of its component molecules. The strength of these interactions determine the value of  $A_{ex}$  [32]. 4MBS and PHS do not form monolayer, hence  $A_x$  remains zero. Figure 6 shows the variation of  $A_{ex}$  as a function of surface pressure for mixed monolayer of 4MBS/DPPC and PHS/DPPC. The negative value of  $A_{ex}$  indicates that the components are having an attractive force between them [45]. That is, the binary monolayer is condensing. From the plots, it is clear that the mixed Langmuir monolayer is more miscible for 0.1 mole fraction of 4MBS and 0.3 mole fraction of PHS (Fig. 6) in DPPC. At higher surface pressure, the  $A_{ex}$  decreases for 4MBS/DPPC mixed monolayer indicating proper mixing of 4MBS in DPPC. In the case of PHS/DPPC mixed monolayer,  $A_{ex}$  is large for lower surface pressure and decreases for higher surface pressures. The  $A_{ex}$  for the mixed Langmuir monolayer corresponding to  $\chi_{PHS} = 0.3$  had minimum  $A_{ex}$  indicating that is more stable as compared to monolayer with  $\chi_{PHS} = 0.1$  and  $0.2$ .

Variation of excess area and excess Gibb's energy as a function of surface pressure for 4MBS and PHS. Solid line is cue to eye

**Fig. 6** Variation of excess area and excess Gibb's energy as a function of surface pressure for 4MBS and PHS. Solid line is cue to eye



To further understand the monolayer stability, the excess Gibbs free energy is calculated using the equation [45],

$$\Delta G_{ex} = N_A \int (A_{12} - \chi_{DPPC} A_{DPPC} - \chi_x A_x) d\pi \tag{4}$$

where,  $N_A$  is the Avogadro number. Figure 6 shows the variation of  $\Delta G_{ex}$  as a function of surface pressure. The negative value of  $\Delta G_{ex}$  correspond to a stable state [46]. The  $\Delta G_{ex}$  value was minimum for 0.1 mole fraction of 4MBS in DPPC. As the composition of 4MBS in the DPPC monolayer increases, the  $\Delta G_{ex}$  values increase, indicating that the stability of the binary monolayer is decreasing.

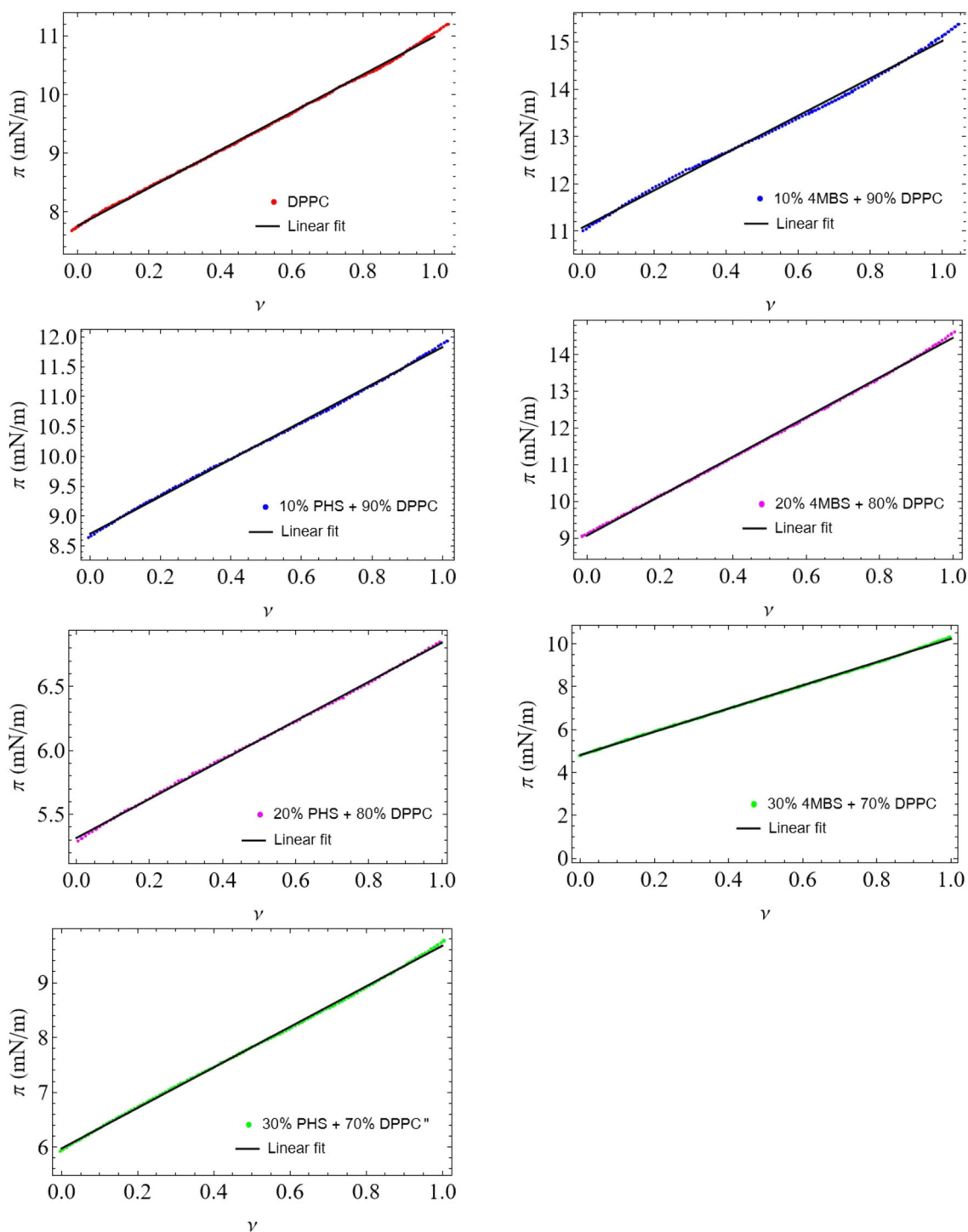


**Fig. 7** Variation of surface pressure as a function of area fraction  $\nu$  for different compositions of 4MBS/DPPC and PHS/DPPC mixed monolayers in the LE-LC coexistence region. The solid line is the linear fit to the data



On the other hand for the mixed monolayer of PHS/DPPC,  $\Delta G_{ex}$  decreases with the increase in the relative mole fraction of PHS (see the Fig. 6). This indicates that, at this 0.3 mole fraction, the monolayer is highly stable compared to monolayers with  $\chi_{PHS}$  of 0.1 and 0.2.

The transition of a monolayer from a disordered LE phase to an ordered LC phase is expected to be a first order phase transition. The  $\pi - A_m$  isotherm of pure and mixed monolayers of DPPC shows a non horizontal slope in the coexistence region. Eiji Hatta et al. explained the non-horizontal slope as a consequence of the lateral molecular density ( $\rho$ )—2D strain ( $\epsilon_s$ ) coupling and the lateral molecular density ( $\rho$ ) – collective chain tilt ( $\theta$ ) contribution to the excess energy [13]. They analysed the phenomenological Landau free energy described by the equation [13],

$$\Delta G(\pi, T) = \frac{1}{2}a(T - T_0)\rho^2 + \frac{1}{4}B\rho^4 + \frac{1}{6}C\rho^6 + \frac{1}{2}K_\theta\theta^2 + \left(\frac{K_0\epsilon^2}{2}\right)\left(\frac{1 + \gamma_0}{1 - \nu}\right) + d\rho^2\theta + e\rho^2\epsilon_s \tag{5}$$

where  $a$ ,  $B$ , and  $C$  are coefficients which are assumed to be independent of temperature and surface pressure.  $T_0$  is the equilibrium transition temperature,  $K_0$  and  $K_\theta$  are the elastic modulus of the LE phase and orientational elastic constant, respectively,  $\gamma_0 = \left(\frac{4}{3}\right)\left(\frac{\mu_0}{K_0}\right)$ , where  $\mu_0$  is the shear modulus of LE phase. The area fraction corresponding to the LC phase with respect to the total area is given by  $\nu = \frac{A_m - A_{LE}}{A_{LC} - A_{LE}}$ . Thus  $\nu$  varies from 0 to 1, where  $\nu = 0$  corresponds to the pure LE phase and  $\nu = 1$  corresponds to the pure LC phase. Raghavendra et al. [19] have derived an equation for surface pressure  $\pi$  as linear function of area fraction  $\nu$  given by

$$\pi = m \nu + \text{constant} \tag{6}$$

Here,  $m = \frac{B\beta\rho^2}{a\frac{dT_c}{d\pi_c}}$ , where  $\beta = \frac{2e^2}{|B|K_0}$  [19]. The variation of surface pressure in the LE–LC coexistence region is plotted as a function of area fraction  $\nu$  (Fig. 7) and is fitted with Eq. 6. For all the compositions of 4MBS and PHS, we find that in coexistence region the surface pressure ( $\pi$ ) linearly varies as a function of  $\nu$ . The slope of the curve is related to the  $\rho - \epsilon_s$  coupling constant ( $e$ ) and is found to be different for various relative composition of 4MBS and PHS. The slope is evaluated from the fit parameters and the value of  $\frac{e^2}{a}$  is calculated for the mixed Langmuir monolayers with different compositions using the equation [19],

$$\frac{e^2}{a} = \frac{mK_0\frac{dT_c}{d\pi_c}}{2\rho^2} \tag{7}$$

where the value of  $\frac{dT_c}{d\pi_c} = 2.35 \text{ mNm}^{-1}\text{K}^{-1}$  for DPPC monolayer [17],  $K_0$  is the compression modulus in the LE phase and the lateral molecular density,  $\rho = \rho_{LC} - \rho_{LE}$ . The values of  $K_0$  and  $\rho$  obtained from fit parameters are tabulated in Table 1.

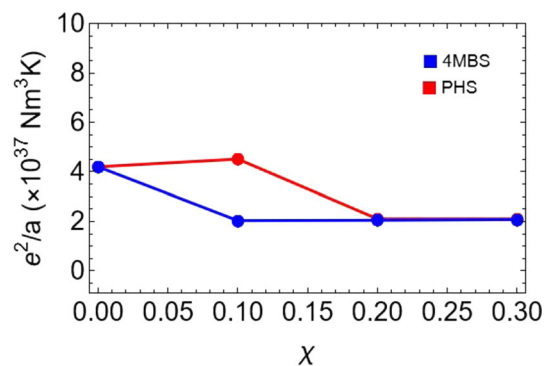
The  $\frac{e^2}{a}$  values for different composition of 4MBS and PHS in DPPC are shown in Fig. 8. From this, it can be noted that the  $\rho - \epsilon_s$  coupling constant ( $e$ ) depends on the composition of the binary monolayer. It is observed that the coupling strength is less for  $\chi_{4MBS} = 0.1$  and then increases slightly for higher concentrations. In the case of PHS/DPPC monolayer, the coupling constant decreases for  $\chi_{PHS} = 0.3$ . The lower value of  $\frac{e^2}{a}$  indicates increased molecular packing[19]. This supports the increased miscibility and stability of the mixed Langmuir monolayer for higher mole fraction of PHS compositions (Fig. 8).

**Table 1** Calculated values of  $K_0$  and  $\rho$  for various compositions of 4MBS and PHS in the mixed monolayer

$\chi$	4MBS		PSP	
	$K_0$ (mNm <sup>-1</sup> )	$\rho$ ( $\times 10^{-3} \text{ \AA}^{-2}$ )	$K_0$ (mNm <sup>-1</sup> )	$\rho$ ( $\times 10^{-3} \text{ \AA}^{-2}$ )
0.1	30.97	3.59	37.79	2.36
0.2	29.56	4.07	29.51	2.14
0.3	26.49	3.84	34.26	3.58

For the monolayer of pure DPPC,  $K_0 = 39.05 \text{ mNm}^{-1}$  and  $\rho = 2.52 \times 10^{-3} \text{ \AA}^{-2}$

**Fig. 8** Variation of  $\frac{e^2}{a}$  values of LE–LC coexistence region of mixed monolayers for mole fraction ( $\chi$ ) of 4MBS and PHS in DPPC monolayer. Solid line is a cue to eye



## 4 Conclusions

We have studied the effect of the stigmaterol-based mesogen 4MBS and phytosphingosine (PHS) on the Langmuir monolayer of DPPC using surface manometry technique. The analysis of the thermodynamical quantities like excess area  $A_{ex}$  and excess Gibbs free energy  $\Delta G_{ex}$  show that the increased composition of 4MBS in the binary monolayer decreases the miscibility and stability of the monolayer but for PHS, increase in composition of PHS (till 0.3 mole fraction) in DPPC increases the miscibility and stability of the mixed monolayer. The analysis of the BAM images of 4MBS/DPPC mixed monolayers have shown that the addition of 4MBS enhances the formation of bright multilobed domains of DPPC. From the analysis of LE–LC coexistence region, it is found that 4MBS increases the coexistence region of DPPC monolayer, unlike other stigmaterol derivatives[47]. Our studies also show that the  $\rho - \epsilon_s$  coupling strength is less for the DPPC monolayer having 0.1 mole fraction of 4MBS and for 0.3 mole fraction of PHS, which again confirms the increased miscibility and stability for this composition.

**Acknowledgements** Mahesha acknowledges DST for INSPIRE fellowship, BK acknowledges VGST, Government of Karnataka for research grants.

**Data Availability** Data available on request from the author.

## References

1. J.H. Borrell, O. Domenech, K.M.W. Keough, Membrane protein–lipid interactions (2016). <https://doi.org/10.1007/978-3-319-30277-5>
2. S.J. Singer, G.L. Nicolson, The fluid mosaic model of the structure of cell membranes. *Science* **175**(4023), 720–31 (1972). <https://doi.org/10.1126/science.175.4023.720>
3. R.P. Giri, A. Chakrabarti, M.K. Mukhopadhyay, Cholesterol-induced structural changes in saturated phospholipid model membranes revealed through x-ray scattering technique. *J. Phys. Chem. B* **121**(16), 4081–4090 (2017). <https://doi.org/10.1021/acs.jpcc.6b12587>
4. Kumar B. Imranpasha, S.L.N. Rao, Interaction of  $\beta$  - N - oxalyl - L -  $\alpha$ ,  $\beta$  - diaminopropionic acid (ODAP) with Langmuir monolayers of DPPC, DPPG and cholesterol. *AIP Conf. Proc.* **2265**(1), 030041 (2020). <https://doi.org/10.1063/5.0016881>
5. A.S. Luviano, J. Campos-Terán, D. Langevin, R. Castillo, G. Espinosa, Mechanical properties of dppc-pope mixed langmuir monolayers. *Langmuir* **35**(51), 16734–16744 (2019). <https://doi.org/10.1021/acs.langmuir.9b02995>
6. H. Mohwald, Phospholipid and phospholipid-protein monolayers at the air/water interface. *Ann. Rev. Phys. Chem.* **41**(1), 441–476 (1990). <https://doi.org/10.1146/annurev.pc.41.100190.002301>
7. C. Pereira-Leite, D. Lopes-de-Campos, P. Fontaine, I.M. Cuccovia, C. Nunes, S. Reis, Licofelone-dppc interactions: putting membrane lipids on the radar of drug development. *Molecules* **24**(3), 516 (2019)
8. G. Van Meer, D.R. Voelker, G.W. Feigenson, Membrane lipids: where they are and how they behave. *Nat. Rev. Mol. Cell Biol.* **9**(2), 112–124 (2008)
9. G. Ma, H.C. Allen, Condensing effect of palmitic acid on dppc in mixed langmuir monolayers. *Langmuir* **23**(2), 589–597 (2007). <https://doi.org/10.1021/la061870i>
10. E.S. Brown, Isolation and assay of dipalmityl lecithin in lung extracts. *Am. J. Physiol.-Legacy Content* **207**(2), 402–406 (1964). <https://doi.org/10.1152/ajplegacy.1964.207.2.402>
11. M. Gang, C.A. Heather, Dppc langmuir monolayer at the air-water interface: Probing the tail and head groups by vibrational sum frequency generation spectroscopy. *Langmuir* **22**(12), 5341–5349 (2006). <https://doi.org/10.1021/la0535227>

12. A. Aroti, E. Leontidis, E. Maltseva, G. Brezesinski, Effects of hofmeister anions on dppc langmuir monolayers at the air-water interface. *J. Phys. Chem. B* **108**(39), 15238–15245 (2004). <https://doi.org/10.1021/jp0481512>
13. E. Hatta, K. Nihei, Emergence of a linear slope region of the isotherm in the first-order liquid-expanded-liquid-condensed phase transition in langmuir monolayers. *Phys. Rev. E* **100**(2), 022801 (2019). <https://doi.org/10.1103/PhysRevE.100.022801>
14. N. Pallas, B. Pethica, Liquid-expanded to liquid-condensed transition in lipid monolayers at the air/water interface. *Langmuir* **1**(4), 509–513 (1985). <https://doi.org/10.1021/la00064a019>
15. Y. Hifeda, G. Rayfield, Evidence for first-order phase transitions in lipid and fatty acid monolayers. *Langmuir* **8**(1), 197–200 (1992). <https://doi.org/10.1021/la00037a036>
16. J. Israelachvili, Self-assembly in two dimensions: surface micelles and domain formation in monolayers. *Langmuir* **10**(10), 3774–3781 (1994). <https://doi.org/10.1021/la00022a062>
17. O. Albrecht, H. Gruler, E. Sackmann, Polymorphism of phospholipid monolayers. *J. Physique* **39**(3), 301–313 (1978). <https://doi.org/10.1051/jphys:01978003903030100>
18. L.R. Arriaga, I. López-Montero, J. Ignés-Mullol, F. Monroy, Domain-growth kinetic origin of nonhorizontal phase coexistence plateaux in langmuir monolayers: Compression rigidity of a raft-like lipid distribution. *J. Phys. Chem. B* **114**(13), 4509–4520 (2010). <https://doi.org/10.1021/jp9118953>
19. Kumar B. Raghavendra, S.N. Chari., Effect of  $\gamma$ -oryzanol on the le–lc phase coexistence region of dppc langmuir monolayer. *The Journal of Membrane Biology*, 1–10 (2023). <https://doi.org/10.1007/s00232-023-00288-8>
20. K. Simons, E. Ikonen, Functional rafts in cell membranes. *Nature* **387**(6633), 569–572 (1997)
21. D. Lingwood, K. Simons, Lipid rafts as a membrane-organizing principle. *Science* **327**(5961), 46–50 (2010)
22. Y. Su, Q. Li, L. Chen, Z. Yu, Condensation effect of cholesterol, stigmaterol, and sitosterol on dipalmitoylphosphatidylcholine in molecular monolayers. *Colloids and Surfaces A* **293**(1–3), 123–129 (2007)
23. R. Ashraf, H.N. Bhatti, Chapter 10 - stigmaterol, in *A Centum of Valuable Plant Bioactives*. ed. by M. Mushtaq, F. Anwar (Academic Press, 2021), pp.213–232. <https://doi.org/10.1016/B978-0-12-822923-1.00019-4>
24. C. Bernsdorff, R. Winter, Differential properties of the sterols cholesterol, ergosterol,  $\beta$ -sitosterol, trans-7-dehydrocholesterol, stigmaterol and lanosterol on dppc bilayer order. *J. Phys. Chem. B* **107**(38), 10658–10664 (2003). <https://doi.org/10.1021/jp034922a>
25. A. Rawlings, Trends in stratum corneum research and the management of dry skin conditions. *Int. J. Cosmetic Sci.* **25**(1–2), 63–95 (2003)
26. H.K. Choi, Y.H. Cho, E.O. Lee, J.W. Kim, C.S. Park, Phytosphingosine enhances moisture level in human skin barrier through stimulation of the filaggrin biosynthesis and degradation leading to nmf formation. *Arch. Dermatol. Res.* **309**, 795–803 (2017)
27. T. Pavicic, U. Wollenweber, M. Farwick, H. Korting, Anti-microbial and-inflammatory activity and efficacy of phytosphingosine: an in vitro and in vivo study addressing acne vulgaris. *Int. J. Cosmetic Sci.* **29**(3), 181–190 (2007)
28. A. Sigruener, V. Tarabin, G. Paragh, G. Liebisch, T. Koehler, M. Farwick, G. Schmitz, Effects of sphingoid bases on the sphingolipidome in early keratinocyte differentiation. *Exp. Dermatol.* **22**(10), 677–679 (2013)
29. S. Vanishree Bhat, K. Swamynathan, S. Kumar, Synthesis and mesomorphic characterization of novel liquid crystals derived from bioactive natural sterols. *J. Mol. Liquids* **326**, 115216 (2021). <https://doi.org/10.1016/j.molliq.2020.115216>
30. V. Bhat, K. Swamynathan, V. Raghunathan, S. Kumar, Synthesis and mesomorphic characterization of novel amphotropic steroidal esters. *New Journal of Chemistry* **47**, (2023). <https://doi.org/10.1039/D2NJ05562G>
31. G.L. Gaines Jr., *Insoluble monolayers at liquid-gas interfaces* (Wiley, New York, 1966)
32. K. Gong, S.-S. Feng, M.L. Go, P.H. Soew, Effects of ph on the stability and compressibility of dppc/cholesterol monolayers at the air-water interface. *Colloids and Surfaces A: Physicochemical and Engineering Aspects* **207**(1–3), 113–125 (2002). [https://doi.org/10.1016/S0927-7757\(02\)00043-2](https://doi.org/10.1016/S0927-7757(02)00043-2)
33. G.L. Gaines Jr., Thermodynamic relationships for mixed insoluble monolayers. *Journal of colloid and interface science* **21**(3), 315–319 (1966). [https://doi.org/10.1016/0095-8522\(66\)90015-8](https://doi.org/10.1016/0095-8522(66)90015-8)
34. B. Gzyl, M. Paluch, Monolayers of lipids at the water-air interface. *Trends Colloid Interface Sci.* **XVII**, 60–63 (2004)
35. D. Andelman, F. Brogård, J.-F. Joanny, Phase transitions in langmuir monolayers of polar molecules. *J. Chem. Phys.* **86**(6), 3673–3681 (1987). <https://doi.org/10.1063/1.451970>
36. K. Sabatini, J.-P. Mattila, P.K. Kinnunen, Interfacial behavior of cholesterol, ergosterol, and lanosterol in mixtures with dppc and dmpe. *Biophys. J.* **95**(5), 2340–2355 (2008). <https://doi.org/10.1529/biophysj.108.132076>
37. K. Hac-Wydro, P. Wydro, A. Jagoda, J. Kapusta, The study on the interaction between phytosterols and phospholipids in model membranes. *Chem. Phys. Lipids* **150**(1), 22–34 (2007). <https://doi.org/10.1016/j.chemphyslip.2007.06.211>
38. A. Lucero, M.R. Rodríguez Niño, A.P. Gunning, V.J. Morris, P.J. Wilde, J.M. Rodríguez Patino, Effect of hydrocarbon chain and ph on structural and topographical characteristics of phospholipid monolayers. *J. Phys. Chem. A B* **112**(25), 7651–7661 (2008). <https://doi.org/10.1021/jp8013157>
39. D.-M. Telesford, D. Verreault, V. Reick-Mitrisin, H.C. Allen, Reduced condensing and ordering effects by 7-ketocholesterol and 5 $\beta$ , 6 $\beta$ -epoxycholesterol on dppc monolayers. *Langmuir* **31**(36), 9859–9869 (2015). <https://doi.org/10.1021/acs.langmuir.5b02539>
40. K. Klopfer, T. Vanderlick, Isotherms of dipalmitoylphosphatidylcholine (dppc) monolayers: features revealed and features obscured. *J. Colloid Interface Sci.* **182**(1), 220–229 (1996). <https://doi.org/10.1006/jcis.1996.0454>

41. C.W. McConlogue, T.K. Vanderlick, A close look at domain formation in dppc monolayers. *Langmuir* **13**(26), 7158–7164 (1997)
42. M. Mayer, T. Vanderlick, Calculation of shapes of dipolar domains in insoluble monolayers: analysis of shape stability and transitions. *J. Chem. Phys.* **100**(11), 8399–8407 (1994)
43. D. Keller, J. Korb, H. McConnell, Theory of shape transitions in two-dimensional phospholipid domains. *J. Phys. Chem.* **91**(25), 6417–6422 (1987)
44. M. Mayer, T. Vanderlick, Monte carlo simulation of the shapes of domains in phospholipid monolayers. *Phys. Rev. E* **55**(1), 1106 (1997)
45. P. Dynarowicz-Latka, K. Kita, Molecular interaction in mixed monolayers at the air/water interface. *Adv. Colloid Interface Sci.* **79**(1), 1–17 (1999). [https://doi.org/10.1016/S0001-8686\(98\)00064-5](https://doi.org/10.1016/S0001-8686(98)00064-5)
46. B. Gzyl, M. Paluch, Properties of insoluble mixed monolayers of lipids at the water/air interface. *Trends Colloid Interface Sci.* **XV**, 22–26 (2001)
47. M. Kodama, O. Shibata, S. Nakamura, S. Lee, G. Sugihara, A monolayer study on three binary mixed systems of dipalmitoyl phosphatidyl choline with cholesterol, cholestanol and stigmasterol. *Colloids Surfaces B* **33**(3), 211–226 (2004). <https://doi.org/10.1016/j.colsurfb.2003.10.008>

Springer Nature or its licensor (e.g. a society or other partner) holds exclusive rights to this article under a publishing agreement with the author(s) or other rightsholder(s); author self-archiving of the accepted manuscript version of this article is solely governed by the terms of such publishing agreement and applicable law.